FBG-Based Mattress for Heart Rate Monitoring in Different Breathing Conditions

Francesca De Tommasi, *Student Member, IEEE*, Carlo Massaroni, *Senior Member, IEEE*, Michele Arturo Caponero, Massimiliano Carassiti, Emiliano Schena, *Senior Member, IEEE*, and Daniela Lo Presti, *Member, IEEE*

***Abstract*—In recent years, extensive investigations have been geared toward finding unobtrusive solutions for monitoring cardiorespiratory activity as an alternative to traditional clinical methods. Among others, the ones based on fiber Bragg grating (FBG) sensors reveal remarkable promise for monitoring respiratory rate (RR) and heart rate (HR). The present study investigates the performance of a mattress based on a 13-FBG array for HR continuous estimation. First, a metrological characterization was performed to assess system characteristics under frequencies simulating typical HR values [i.e., 60, 90, and 120 beats per minute (bpm)]. Then, the proposed device was tested on eight healthy volunteers (both males and females) in the presence of different breathing stages (i.e., quiet breathing and tachypnea) while mimicking common sleeping postures (i.e., supine, left side, and prone). The assessment of HR measurements under different breathing regimes and postures has rarely been addressed in FBG-based technologies. The achieved results suggest that the proposed mattress has promising capability in reliably estimating HR values. These results together with the ones obtained in terms of RR monitoring in a recent study reveal the high potential for monitoring cardiorespiratory activity.**

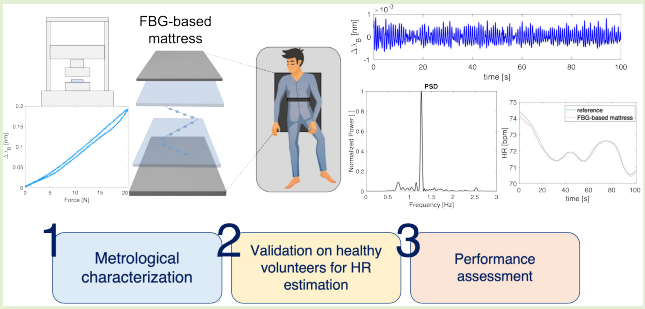

***Index Terms*—Cardiorespiratory monitoring, fiber Bragg grating (FBG) sensors, heart rate (HR) monitoring, smart mattress, unobtrusive monitoring.**

I. Introduction

IN THE last few years, cardiorespiratory diseases have been claiming an impressive number of lives worldwide, with worrying statistics [1], [2], [3], [4]. Cardiac arrest, stroke, chronic obstructive pulmonary disease, and sleep apnea count among the common pathological conditions in this area [5], [6], [7], [8], [9]. The increase in population aging is one of the primary causes of this global burden, as it heightens lifetime exposure to risk drivers [10], [11]. Therefore, chronic illness incidence stands to grow further in the upcoming decades, entailing the inability of healthcare facilities to manage patients adequately. In this framework, home monitoring can be a viable alternative for managing such pathologies, thus reducing hospital admissions and costs associated with their care [12], [13], [14], [15]. This cutting-edge healthcare leads to continuous monitoring of the health status, preventing the occurrence of adverse events and tailoring treatment toward patient's needs. As a result, a great deal of research has been devoted to finding unobtrusive solutions for monitoring cardiorespiratory activity over traditional ones (i.e., electrocardiogram (ECG) and direct respiratory airflow measurements) [16], [17], [18]. In this scenario, wearable and instrumented objects are gaining ground, as huge numbers of scientific papers testify [16], [18], [19], [20], [21], [22], [23], [24]. Chest straps, soft patches attached directly to the skin, instrumented chairs, cushions, and beds can be found in the literature involving the use of different types of sensors [25], [26], [27], [28], [29], [30], [31]. Among others, instrumented mattresses are growing in importance as they allow monitoring subjects in long-term

Manuscript received 2 May 2023; accepted 9 May 2023. Date of publication 16 May 2023; date of current version 29 June 2023. The associate editor coordinating the review of this article and approving it for publication was Prof. Arnaldo G. Leal-Junior. *(Corresponding author: Daniela Lo Presti.)*

This work involved human subjects or animals in its research. Approval of all ethical and experimental procedures and protocols was granted by the University Campus Bio-Medico di Roma under Application No. 27/18 OSS, and performed in line with the Declaration of Helsinki.

Francesca De Tommasi, Carlo Massaroni, Emiliano Schena, and Daniela Lo Presti are with the Unit of Measurements and Biomedical Instrumentation, Departmental Faculty of Engineering, University Campus Bio-Medico di Roma, 00128 Rome, Italy (e-mail: d.lopresti@unicampus.it).

Michele Arturo Caponero is with the ENEA Research Center of Frascati, 00044 Frascati, Italy.

Massimiliano Carassiti is with the Unit of Anesthesia, Intensive Care and Pain Management, School of Medicine, Fondazione Policlinico Universitario Campus Bio-Medico, 00128 Rome, Italy.

Digital Object Identifier 10.1109/JSEN.2023.3275323

This work is licensed under a Creative Commons Attribution 4.0 License. For more information, see https://creativecommons.org/licenses/by/4.0/

scenarios where the detection of physiological changes can be paramount in preventing the outbreak of specific disorders (such as obstructive sleep apnea) [32], [33], [34], [35], [36], [37], [38], [39], [40].

Fiber Bragg grating (FBG) sensors are promising sensing solutions proposed for developing such technologies and tracking both respiratory rate (RR) and heart rate (HR) [22] from the detection of chest wall deformations occurring during inhalation and exhalation phases of a breathing act and thoracic vibrations in response to heart beating (known as seismocardiogram (SCG) [41]). These physiological activities cause periodic perturbation in the FBG output [22], [23]. The adequate postprocessing of signals may further obtain the estimation of RR and HR via strain sensing with the same device. This is one of the reasons for the FBGs success in this field, along with their well-known advantages (e.g., biocompatibility, lightweight, small size, electromagnetic immunity, and multiplexing capabilities [42]). In recent years, FBGs encapsulation in supporting materials (e.g., silicone rubber, resin, and 3-D printing materials) has been proposed to customize developed devices according to the specific application's requirements and to increase their robustness, overcoming the intrinsic fragility [43], [44], [45], [46], [47]. Although various FBG-based wearable solutions exist, only a few explored the possibility of monitoring HR together with RR. Moreover, it is worth noting that their use requires proper wearability for accurate measurements and may constrain the subject's movements. As a consequence, the user's acceptability might be impaired in long-term applications. To overcome these drawbacks, instrumentation of daily-use objects is often favored [27], [32], [33], [34], [35], [36]. However, both in wearable and nonwearable solutions, HR extraction is generally performed only during apnea phases or under quiet breathing (QB) conditions, neglecting estimation in the presence of altered breathing patterns [i.e., tachypnea (T)], which can occur in cardiorespiratory diseases [22], [27], [30], [31], [32], [33], [47], [48].

Recently, we proposed the design, development, and feasibility assessment of an instrumented mattress consisting of multiple FBG sensors embedded in silicone materials for RR estimation by mimicking different sleeping postures [35]. Subjects with different sex and anthropometric characteristics were enrolled in the study, achieving promising results. In this article, we investigate the ability of the same technological solution proposed in [35] but in continuous HR estimation under different breathing conditions (i.e., QB and T) and sleeping postures. The FBG-based mattress assessment on HR monitoring ability, combined with the one already validated for RR estimation, makes the proposed system a valuable solution for cardiorespiratory monitoring.

II. FBG-Based Mattress: System Description, Working Principle, and Metrological Characteristics

A. System Description and FBGs Working Principle

The mattress, proposed in [35], lies in 13 FBGs optically inscribed in the same array (λ_B values over the range 1512–1568 nm, each grating 10 mm long and a distance edge-to-edge of 40 mm), individually encapsulated within a circular-shaped silicone matrix of DragonSkin[1] 10. Once produced, these 13 elements were arranged in a serpentine manner and sandwiched inside two further rectangular silicone layers (DragonSkin30 for the bottom layer and DragonSkin10 for the top layer) measuring 500 × 400 mm, intended to fit the upper torso and mid-torso of the lying subject. Moreover, two sheets of nitrile butadiene rubber (NBR; 500 × 800 mm) were attached to the lower and upper mattress surface through a double-sided adhesive tape to attain a more robust structure (see Fig. 1). Further information about the design and fabrication processes is described in [35]. The sensing core element of the proposed solution is FBG technology. Basically, an FBG consists of a short optical fiber section modified to create a permanent periodic variation of the refractive index along its length. This segment acts as a specific wavelength resonator, reflecting a narrow spectrum centered around the so-called Bragg wavelength (i.e., λ_B) expressed as follows [49]:

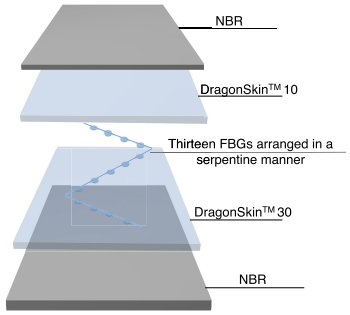

Fig. 1. FBG-based mattress consisting of 13 FBGs, one layer of DragonSkin10, another one of DragonSkin30, and two closing sheets of NBR.

$$\lambda_B = 2 \cdot n_{\text{eff}} \cdot \Lambda \tag{1}$$

where n_{eff} denotes the effective refractive index of the fiber core and Λ is the grating period. When the fiber is thermally or mechanically stressed, λ_B experiences a shift that can be measured to trace the strain (ϵ) or the temperature variation (ΔT) applied. In this study, temperature contributions on the FBGs output can be assumed negligible compared to the one due to the physiological activities as the temperature variations present slow dynamics than the cardiac ones. Moreover, the human body is not in close contact with the sensing elements since the FBGs sensors are sandwiched by additional polymer layers that may dampen the influence of the temperature on the recorded signals (for more details, see [35]).

Nevertheless, FBGs integration within flexible or rigid materials leads to the possibility of their use not only for strain and temperature purposes but also as force sensors, such as in this specific case. Since the mechanical properties of the material selected for encapsulation can affect the metrological properties of the overall sensing element, a characterization process is required to assess them.

B. Metrological Characteristics

When a subject lays down on the mattress, the force applied on its surface is transmitted to the encapsulated FBGs inducing a strain along the longitudinal axis of the grating and causing

[1] Trademarked.

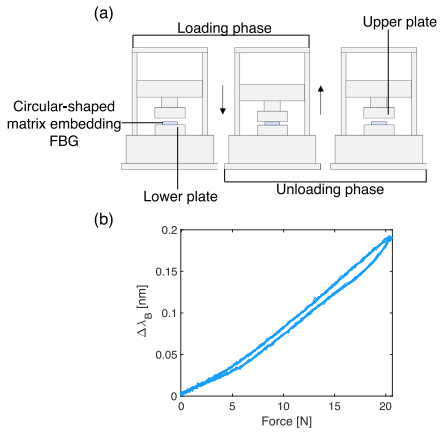

Fig. 2. (a) Positioning of the circular-shaped matrix embedding the FBG between the upper and lower plates of the testing machine and detailing loading and unloading phase of hysteresis loops. (b) Example of hysteresis curve obtained from one of the 13 FBGs.

a shift of λ_B. In [35], a static characterization process was carried out to assess the force sensitivity (S_F) of each of the 13 FBGs encapsulated in soft circular matrices before their integration in the final mattress structure. The results obtained showed S_F values ranging between 10 and 18 pm $\cdot$ N^{-1} (14 pm $\cdot$ N^{-1} of mean value and 2 pm $\cdot$ N^{-1} of standard deviation). Considering the application scenario, the RR and HR monitoring, also dynamic tests at frequencies mimicking typical RR values have been performed in [35] to assess the mean percentage hysteresis error (i.e., $\overline{h_{\text{err}}\%}$), yielding results always below $\leq$18%.

In the present study, we also evaluated $\overline{h_{\text{err}}\%}$ at frequencies simulating HR values of 60, 90, and 120 beats per minute (bpm) to cover the proposed system when used as a device for cardiorespiratory monitoring. To perform the hysteresis analysis, each circular-shaped matrix embedding of the FBG was placed between the upper and lower plates of a testing machine (model 3365, Instron[2], Norwood, MA, USA), and loading and unloading phases of each loop were performed as compression tests between 0 and 20 N and 20 and 0 N, respectively (see Fig. 2). Seven hysteresis cycles were completed for each frequency and for all 13 sensors. A sampling rate of 100 Hz was set to collect both tensile machine and FBG outputs. The percentage hysteresis error (i.e., $h_{\text{err}}\%$) was calculated according to the following equation:

$$h_{\text{err}}\% = \frac{\Delta\lambda_B^{\text{loading}} - \Delta\lambda_B^{\text{unloading}}}{\max\left(\Delta\lambda_B^{\text{loading}}\right)} \cdot 100 \qquad (2)$$

where $\Delta\lambda_B^{\text{loading}} - \Delta\lambda_B^{\text{unloading}}$ represents the highest $\Delta\lambda_B$ gap between the loading and unloading phases when the same input force is applied and $\max(\Delta\lambda_B^{\text{loading}})$ denotes the maximum $\Delta\lambda_B$ reached during the loading phase. Then, for each FBG, the $\overline{h_{\text{err}}\%}$ value was computed as the mean $h_{\text{err}}\%$ values across the seven loops for velocities mimicking HR of 60, 90, and 120 bpm. The results in terms of $\overline{h_{\text{err}}\%}$ and uncertainty obtained for each FBG and HR value are reported in Fig. 3. As can be seen, the maximum $\overline{h_{\text{err}}\%}$ values were always lower than 20% for all HR values.

[2]Registered trademark.

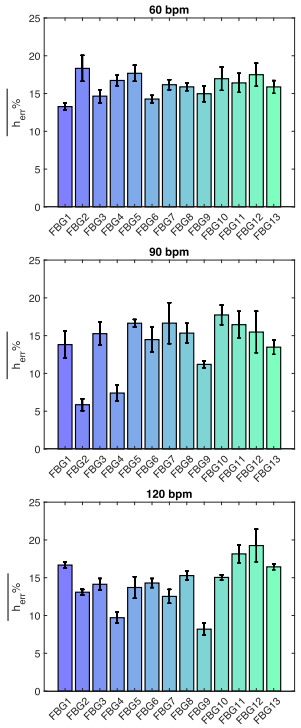

Fig. 3. Mean percentage hysteresis error (i.e., $\overline{h_{\text{err}}\%}$) and the related uncertainty obtained for each FBG (from FBG1 to FBG13) and all the simulated HR values (i.e., 60, 90, and 120 bpm).

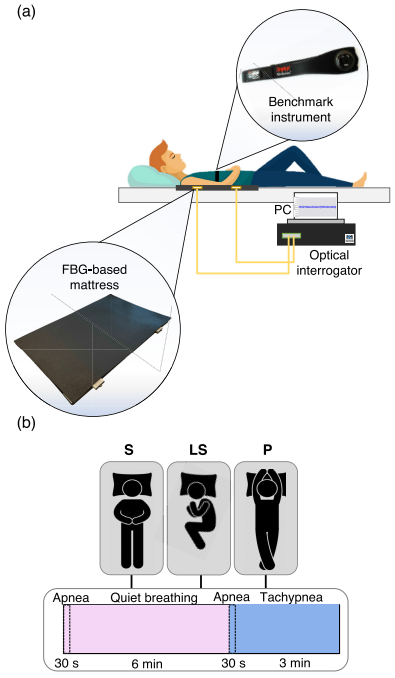

Fig. 4. (a) Schematic of the experimental setup consisting of stiff surface, FBG-based mattress, benchmark instrument, PC, and optical interrogator. (b) Simulated positions (i.e., S, LS, and P) and performed protocol for each one.

III. FBG-Based Mattress: Feasibility Assessment for HR Estimation

Once the metrological characterization in terms of response to cyclic force inputs at frequencies simulating typical HR values, the feasibility assessment of the FBG-based mattress was carried out as follows.

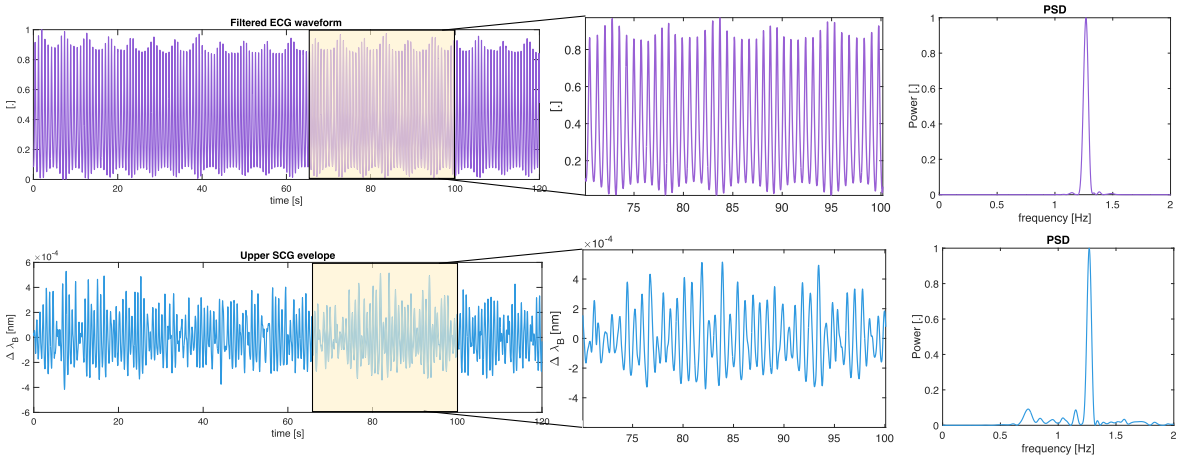

Fig. 5. Left: example of a filtered ECG waveform and upper SCG envelope from the most informative FBG sensor during 120 s of QB stage. Right: zoomed-in view of 30-s window of the ECG and SCG along with the related PSD.

A. Experimental Setup and Protocol

Eight healthy volunteers (three males and five females) were enrolled in this study. The recruitment was accomplished in adherence to the Declaration of Helsinki and after the ethics committee approval of our institution (ST-UCBM 27/18 OSS). The participants' demographic and anthropometric characteristics were collected and given as a mean and standard deviation: 27 ± 3 years old, a body mass of 67 ± 15 kg, and a height of 170 ± 8 cm. The experiments were performed in a laboratory environment, whereby the FBG-based mattress was initially placed on a stiff surface (dimensions compatible with those of a single bed). Each subject was invited to lie down on this support while keeping relaxed on the mat and to follow this protocol: 30 s of apnea, 6 min of QB, 30 s of apnea, and 3 min of T. This protocol was repeated thrice for each volunteer under three different sleeping postures supine (S), left side (LS), and prone (P) positions (the total acquisition of 30 min). During the experiments, the FBG-based mattress was physically connected to an optical interrogator (i.e., si255, Hyperion Platform, Micro Optics Inc., Atlanta, GA, USA) to record its output at a sampling rate of 1 kHz. In the meantime, a wearable chest band (BioHarness 3.0, Zephyr Technology, Medtronic, Fridley, MA, USA) was used as a benchmark to collect ECG and breathing waveforms at 250 and 25 Hz, respectively. Fig. 4 shows in outline the experimental setup, the simulated positions, and the applied protocol.

B. Data Analysis

MATLAB was used to postprocess data through a dedicated algorithm. First, the data were synchronized considering the end-expiratory peak after apnea, for each subject. Then, ECG data and FBG-based mattress were sorted according to the position (i.e., S, LS, and P). For each of them, data were split into two stages: a first part considering the 6 min of QB and a second part taking over 3 min of T. Afterward, four main processing steps were implemented for each position (S, LS, and P) and condition (QB and T) to retrieve HR values from both the benchmark system and FBG-based mattress and assess performance. Sections III-B.1–III-B.4 detail each of them.

1) Filtering Process: ECG data were first-order Butterworth filtered with a lower cutoff frequency of 0.7 Hz and a higher one of 2 Hz to emphasize the R peaks in the traces (the first subplot on the LS in Fig. 5). $\Delta\lambda_B$ signals collected from the 13 FBGs were processed using a third-order passband filter with cutoff frequencies of 3–10 Hz for QB and 5–10 Hz for T to obtain the SCG waveforms. The selection of 5 Hz as a low cutoff frequency for T is warranted since, during T, an overlap between the high-frequency respiratory and low-frequency cardiac components can occur. Then, the envelope function was used to analyze the 13 SCG signals and identify the peaks associated with aortic valve opening events that generally occur 200 ms after the R peaks on ECG on the upper envelope trace filtered. Then, a first-order passband filter (0.7 and 2 Hz) was applied to the extracted upper SCG envelopes (see the second subplot in the left of Fig. 5).

2) Automatic Selection of the Most Informative FBG: Welch's estimator was used to calculate the power spectral density (PSD) of all the 13 $\Delta\lambda_B$'s for each position and condition. For HR estimation, only the FBG with the highest power spectrum was considered, in accordance with [35].

3) Continuous HR Estimation: The filtered data from the most informative FBG and those from ECG were split into sliding windows of 30 s moving every 1 s and analyzed in the frequency domain to estimate the PSD plots using Welch's overlapped method (see the plots in the right of Fig. 5. For each window, the frequency value at which the maximum power occurred was identified (i.e., dominant frequency $f_{\max}$), and HR values were extracted as follows:

$$\mathrm{HR} = 60 \cdot f_{\max}. \tag{3}$$

Possible outliers in HR values considered as values greater than two times the standard deviation from the mean were identified and removed in both ECG and the selected FBG signals.

4) Performance Assessment: To evaluate the performance of the FBG-based mattress in HR estimation for each subject, position (i.e., S, LS, and P), and condition (i.e., QB and T),

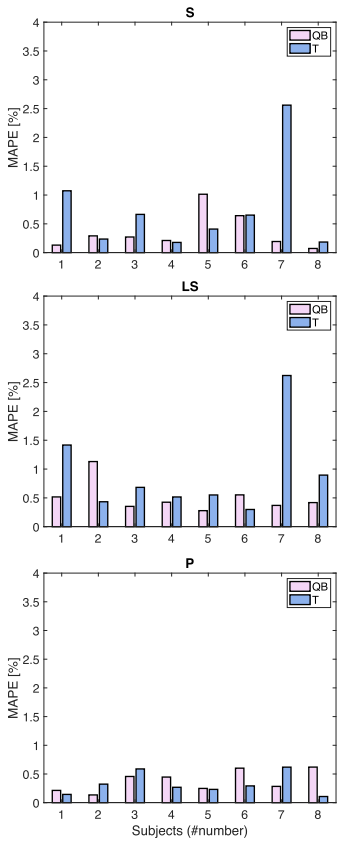

Fig. 6. MAPE values clustered in three bar plots according to the simulated position (i.e., S, LS, and P). In each plot, values found are reported for each subject and marked in different color bars for QB (pink bar) and T (blue bar).

the mean absolute percentage error (MAPE) was calculated according to

$$\text{MAPE}[\%] = \frac{1}{n}\sum_{k=1}^{n}\frac{\left|\text{HR}_k^{\text{mattress}} - \text{HR}_k^{\text{ref}}\right|}{\text{HR}_k^{\text{ref}}} \cdot 100 \qquad (4)$$

where $\text{HR}_k^{\text{mattress}}$ and HR_k^{ref} denote the HR values estimated in the kth window for the FBG-based mattress and reference, respectively, and n is the number of windows. Furthermore, the agreement between the two systems was quantified through the Bland–Altman analysis, which provides the mean of difference (MOD) and limits of agreement (LOAs). In this analysis, HR values were considered separately in the two breathing conditions (i.e., QB and T) and considering together QB and T data, for each simulated position (i.e., S, LS, and P).

C. Results

MAPE values are shown in Fig. 6 using bar plots (one for each simulated sleeping position) where QB and T conditions are marked by pink and blue bars, respectively. Considering each body position, the best results were obtained for the P position, where no considerable differences were found comparing QB and T phases (a maximum of 0.6% both in QB and T). Otherwise, a maximum MAPE of 1.0% for QB and 2.6% for T was found for the S position. It is worth noting that, except for Subject #5 in QB and Subject #7 in T, MAPE values are always <0.6% for QB and <1.0% for T. Similar MAPE values were obtained in the case of LS (up to 1.1% in QB and 2.6% in T). Once again, except for Subject 7 in T, MAPE values were always <1.1%. However, results reached under all three positions are promising. Moreover, we can state that the proposed system showed better results in QB than T. Indeed, no appreciable differences were found in QB considering all three body positions (MAPE values always <1%), while values in T are higher than two times the ones obtained in QB (MAPE values <2.6 %).

TABLE I
BLAND–ALTMAN: MOD ± LOAS OBTAINED FOR S, LS, AND P POSITION IN QB, T, AND CONSIDERING THE COMBINED CONDITIONS (QB + T)

	MOD ± LOAs [bpm]		
	QB	T	QB+T
S	-0.08±1.9	-0.03±3.5	-0.07±2.5
LS	-0.11±2.0	-0.30±3.6	-0.17±2.6
P	-0.09±1.6	-0.08±1.4	-0.08±1.5

With respect to Bland–Altman plots obtained for S, LS, and P positions for QB [Fig. 7(a)] and T [Fig. 7(b)], MOD values were comparable and close to zero along the three positions for both QB and T. In QB, LOAs are similar across S, LS, and P (up to 2.0 bpm for LS). Worst LOAs values were achieved in T for S and LS (up to 3.6 bpm). Instead, for P, similar values were found for both QB and T. Table I summarizes the MOD and LOAs obtained in S, LS, and P for QB and T, and considering the two combined conditions (QB + T), better performance was experienced under P sleeping posture (-0.08 ± 1.5 bpm).

IV. DISCUSSION AND CONCLUSION

The FBG-based mattress appears as a valuable alternative for long-term cardiorespiratory monitoring compared to conventional methods. In a previous study, we reported its design, development, and preliminary validation for RR estimation [35]. This solution consists of 13 FBGs embedded in a circular-shape matrix and disposed serpentine-like within four rectangular silicone and NBR layers for conferring more robustness to the overall structure. The mattress dimension and the sensors arrangement allow for monitoring individuals exhibiting different heights, body mass, and taking up various postures.

In the present work, we investigated the possibility of estimating HR to gather information about the device's suitability for simultaneously monitoring HR under breathing. The results obtained, combined with those already studied in [35] for RR monitoring, suggest a high capability of the proposed device to fulfill as a system for cardiorespiratory monitoring, which is a key aspect in fostering the treatment and diagnosis of chronic diseases. Before performing the validation of the system performance on healthy volunteers, a metrological characterization was carried out to assess $\overline{h_{\text{err}}\%}$ for each FBG under velocities simulating typical HR values (i.e., 60, 90, and 120 bpm). This process establishes whether the system can pursue periodic variations of the parameter in question. Results showed a maximum $\overline{h_{\text{err}}\%}$ lower than 20%. The hysteresis assessment is commonly neglected in studies dealing

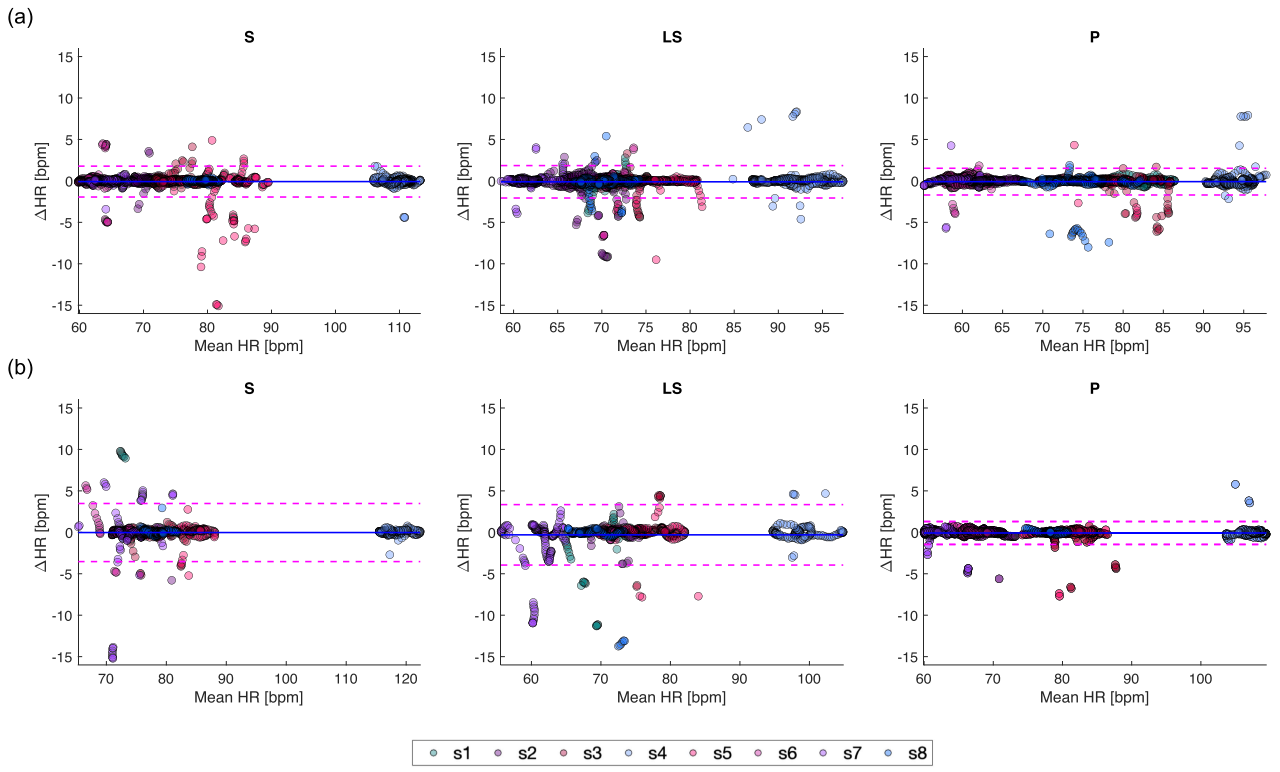

Fig. 7. Bland–Altman plots showing the bias between $HR_i^{mattress}$ and $HR_i^{reference}$ (i.e., ΔHR [bpm]) calculated for S, LS, and P positions in (a) QB and (b) T. In each plot, the MOD is reported with a continuous blue line and LOAs with pink dashed lines.

with mattresses for cardiorespiratory monitoring. Compared to other FBG-based wearable devices, $\overline{h_{err}\%}$ values obtained are comparable or even better than the ones reported in [26] and [31] (up to 25% in [26] and 30% in [31]). Then, the feasibility assessment was accomplished by enrolling eight healthy subjects (both males and females), invited to lie down on the mat and simulate different breathing conditions (QB and T) in different postures (i.e., S, LS, and P) for a total of 30 min of acquisition per each subject. HR investigations with FBG technologies are usually performed when the subject holds his breath since its estimation is facilitated by the a priori exclusion of respiratory components [22], [30], [31], [48]. Few studies include QB patterns, but over a limited period [27], [32], [33], [47]. To date, the literature lacks research proposing HR extraction during breathing conditions, especially in T since the overlap between breathing frequency components and cardiac ones in the signal output occurs more heavily, making its estimation very challenging. A first attempt was done in [26] with a soft patch, but it was performed considering only 60 s of acquisition. No studies exploring this aspect with instrumented mattresses were found. Our investigation overcomes this limitation, as we also considered T breathing stages, which may occur in patients affected by chronic pathologies [18]. Furthermore, women were also included in this study and in a higher rate than men (5 versus 3). For performance validation, this is quite unusual since the enrolment generally includes men or at least in a higher percentage than females [27], [28], [31], [32], [33], [44]. To assess the feasibility of the proposed solution, HR values were estimated also considering different sleeping postures (i.e., S, LS, and P), unlike studies proposed in [27] and [33] carrying out experiments only in the S position. Compared to our previous study [35], we excluded the HR estimation for the right-side position as in this case the heart is far from the instrumented mattress surface. In the future, we envisage implementing a posture recognition algorithm.

Data collected were automatically postprocessed in the frequency domain by computing Welch's method to first select the most informative sensor (for each position—S, LS, and P—and breathing condition—QB and T) and second to estimate HR by splitting the signal from the selected one into sliding windows of 30 s moving every 1 s. The proposed selection algorithm is the same implemented in our previous work [35] for RR. As a result, in the future, both RR and HR can be assessed using this approach, thereby reducing the computational cost required for their evaluation. MAPE values obtained were less than 1.1% in the case of QB for all the simulated positions (Fig. 6) better than the one found in [30] obtained for an FBG-based chest strap during apnea. Instead, in the case of T, MAPE reached up to 2.6% with worse results in the case of S and LS postures. However, it is worth noting that this value was achieved for only one subject (see Fig. 6) for both S and LS, and for the others, MAPE was always below 1.5% (see Fig. 6). The Bland–Altman analysis suggests the reliability of the proposed device in monitoring HR, with MOD values close to 0 and LOAs values lower than 3.6 bpm for T and 2.0 bpm for QB, outperforming the ones of [32] and [33] proposing the use

TABLE II
COMPARISONS WITH OTHER SIMILAR STUDIES AVAILABLE IN THE LITERATURE BASED ON MATTRESSES FOR HR MONITORING

Reference	Sensing technology	Number of subjects enrolled;acquisition time; body position (if specified)	Analysis and reference device	Results
[32]	One FBG attached on a plexiglass board	12 healthy subjects 5 min of acquisition time Supine position	Time domain analysis to estimate HR (peaks detection to find the local maxima) ECG used as benchmark (Invivo, Gainesville)	Bland-Altman (MOD±LOAs): -0.01±1.82 bpm
[33]	One FBG attached on a plexiglass board	12 healthy subjects 5 min of acquisition time Supine position	Time domain analysis to estimate HR (peaks detection to find the local maxima) ECG used as benchmark (Invivo, Gainesville)	Bland-Altman (MOD±LOAs): 0.01±1.64 bpm
[36]	Twelve FBGs positioned on the bed mattress surface	NA*	Frequency domain analysis (Fast Fourier Transform -FFT) to estimate HR Pulse oximeter used as benchmark (NONIN – AVANT 4000)	NA
[37]	Plastic optical fiber	10 participants 90 s of acquisition time Supine position	Frequency domain analysis (Power Spectral Density - PSD) to estimate HR Pulse oximeter used as benchmark (YH303, Yuwell, China)	Absolute error up to 3.4 bpm
[38]	EverOn (EarlySense, Ramat Gan, Israel) Piezoelectric sensors	37 children and 16 adults 1 min of acquisition in sleep lab assessment Position NA 42 patients 6 to 24 hours of acquisition in the intensive care unit (ICU) Supine positions	Time domain analysis (one-minute measurements averaged and compared) to estimated HR; Polysomnography used as a benchmark (RR Embla N700) for in sleep lab ECG used as a benchmark (Datex/Ohmeda, GE medical, Madison, WI, USA) for ICU patients	HR accuracy of 94.4% for adults and 91.4% for children in the case of sleep lab and 94.0% for ICU measurements. MAPE of 3% for adults and 5% for children in the case of a sleep lab and equal to 3% for ICU patients.
[39]	Air-filled pad connected to a pressure sensor	31 patients and 6 healthy volunteers (mostly composed by males) Acquisition time NA Position NA	Time domain analysis (one-night averaged value of HR estimated) ECG used as a benchmark (recorded by Somtè polysomnography system)	Bland-Altman (MOD±LOAs): 0.8±3.5 bpm (60% of data excluded by the algorithm)
[40]	Emfit Ltd (Vaajakoski, Finland) Ferroelectric sensors	34 patients 1 h for each enrolled subject Supine position	Frequency domain analysis (PSD on overlapping windows) to estimate HR ECG from polysomnography used as benchmark (Embla N700)	Bland-Altman (MOD±LOAs): 0.03±4.4 bpm
Present study	13 FBGs encapsulated in soft circular matrixes of silicone rubber	8 healthy participants 30 min of acquisition time for each subject (i.e., 10 min for each posture by simulating different breathing conditions: 30 s of apnea, 6 min of QB, 30 s of apnea, and 3 min of T) Supine, right side, and prone positions.	Frequency domain analysis (PSD on overlapping window) to estimate HR from the most informative sensor. ECG used as a benchmark (BioHarness 3.0, Zephyr Technology, Medtronic)	Bland-Altman (MOD±LOAs): Supine position for QB:-0.08±1.9 bpm; for T: 0.03±3.5 bpm) Left side for QB:-0.11±2.0 bpm; for T: =-0.30±3.6 bpm Prone position for QB: -0.09±1.6 bpm; for T: =-0.08±1.4 bpm MAPE always lower than 2.6% in all the simulated positions and breathing conditions

*NA: not available

of an FBG attached to a plexiglass board for monitoring HR in the S position (see Fig. 7). Results obtained considering both breathing conditions (i.e., QB + T) reported LOAs up 2.6 bpm compliant with medical device guidelines requiring values below 5 bpm for HR estimation [50]. In general, better performance is achieved in the P position as obtained for RR

in [35]. Overall, no significant differences were found between male (volunteers no. 1, 2, and 5) and female subjects. Table II also reported other comparisons with similar studies available in the literature based on mattresses for HR monitoring. It includes for each of the listed works, the proposed sensing technology, the number of subjects enrolled, the acquisition time and the simulated body positions, the performed analysis, and the presence of any reference device to assess the proposed system performance together with the main results. In Table II, our solution was reported in the last row for easy comparison.

The encouraging achievements reveal the potential of this system for continuous HR measurements that combined with RR measurements performed in [42] establish this device as a promising sensing solution suitable for monitoring cardiorespiratory activity. It is important to point out that the high price and, in some cases (e.g., in wearable solutions), the bulkiness of the interrogation unit can limit its widespread use in daily-life applications. However, in recent years, several advances have been made to reduce its size together with the price, as also testified by the small interrogators commercially available on the market [23], [51], [52]. Although the performance of the small instruments is still lower than bulky ones, we expect powerful advancements in the next future. Moreover, the limited number of subjects enrolled requires further investigation to corroborate these findings.

REFERENCES

[1] N. Townsend et al., "Epidemiology of cardiovascular disease in Europe," *Nature Rev. Cardiol.*, vol. 19, no. 2, pp. 133–143, 2022.

[2] L. J. Laslett et al., "The worldwide environment of cardiovascular disease: Prevalence, diagnosis, therapy, and policy issues," *J. Amer. College Cardiol.*, vol. 60, no. 25, pp. S1–S49, Dec. 2012.

[3] T. Ferkol and D. Schraufnagel, "The global burden of respiratory disease," *Ann. Amer. Thoracic Soc.*, vol. 11, no. 3, pp. 404–406, Mar. 2014.

[4] P. Burney, D. Jarvis, and R. Perez-Padilla, "The global burden of chronic respiratory disease in adults," *Int. J. Tuberculosis Lung Disease*, vol. 19, no. 1, pp. 10–20, Jan. 2015.

[5] G. Savarese, P. M. Becher, L. H. Lund, P. Seferovic, G. M. C. Rosano, and A. J. S. Coats, "Global burden of heart failure: A comprehensive and updated review of epidemiology," *Cardiovascular Res.*, vol. 118, no. 17, pp. 3272–3287, Jan. 2023.

[6] V. L. Feigin et al., "World stroke organization (WSO): Global stroke fact sheet 2022," *Int. J. Stroke*, vol. 17, no. 1, pp. 18–29, Jan. 2022.

[7] T. D. Bradley and J. S. Floras, "Obstructive sleep apnoea and its cardiovascular consequences," *Lancet*, vol. 373, no. 9657, pp. 82–93, Jan. 2009.

[8] D. Adeloye, P. Song, Y. Zhu, H. Campbell, A. Sheikh, and I. Rudan, "Global, regional, and national prevalence of, and risk factors for, chronic obstructive pulmonary disease (COPD) in 2019: A systematic review and modelling analysis," *Lancet Respiratory Med.*, vol. 10, no. 5, pp. 447–458, May 2022.

[9] A. Khokhrina, E. Andreeva, and J.-M. Degryse, "A systematic review on the association of sleep-disordered breathing with cardiovascular pathology in adults," *NPJ Primary Care Respiratory Med.*, vol. 32, no. 1, p. 41, Oct. 2022.

[10] J. Pomerleau, C. Knai, and E. Nolte, "The burden of chronic disease in Europe," in *Caring for People With Chronic Conditions: A Health System Perspective*. 2008, pp. 15–42. [Online]. Available: https://www.nature.com/articles/nature06516

[11] W. Lutz, W. Sanderson, and S. Scherbov, "The coming acceleration of global population ageing," *Nature*, vol. 451, no. 7179, pp. 716–719, Feb. 2008.

[12] G. Paré, M. Jaana, and C. Sicotte, "Systematic review of home telemonitoring for chronic diseases: The evidence base," *J. Amer. Med. Inform. Assoc.*, vol. 14, no. 3, pp. 269–277, May 2007.

[13] B. G. Celler, N. H. Lovell, and J. Basilakis, "Using information technology to improve the management of chronic disease," *Med. J. Aust.*, vol. 179, no. 5, pp. 242–246, Sep. 2003.

[14] M. Ishijima, "Unobtrusive approaches to monitoring vital signs at home," *Med. Biol. Eng. Comput.*, vol. 45, pp. 1137–1141, Sep. 2007.

[15] S. Majumder et al., "Smart homes for elderly healthcare—Recent advances and research challenges," *Sensors*, vol. 17, no. 11, p. 2496, Oct. 2017.

[16] C. Brüser, C. H. Antink, T. Wartzek, M. Walter, and S. Leonhardt, "Ambient and unobtrusive cardiorespiratory monitoring techniques," *IEEE Rev. Biomed. Eng.*, vol. 8, pp. 30–43, 2015.

[17] Y. Guo et al., "A review of wearable and unobtrusive sensing technologies for chronic disease management," *Comput. Biol. Med.*, vol. 129, Feb. 2021, Art. no. 104163.

[18] C. Massaroni, A. Nicolò, D. Lo Presti, M. Sacchetti, S. Silvestri, and E. Schena, "Contact-based methods for measuring respiratory rate," *Sensors*, vol. 19, no. 4, p. 908, Feb. 2019.

[19] S. Choi and Z. Jiang, "A novel wearable sensor device with conductive fabric and PVDF film for monitoring cardiorespiratory signals," *Sens. Actuators A, Phys.*, vol. 128, no. 2, pp. 317–326, Apr. 2006.

[20] E. Piuzzi, S. Pisa, E. Pittella, L. Podestà, and S. Sangiovanni, "Wearable belt with built-in textile electrodes for cardio—Respiratory monitoring," *Sensors*, vol. 20, no. 16, p. 4500, Aug. 2020.

[21] S. Chen, J. Qi, S. Fan, Z. Qiao, J. C. Yeo, and C. T. Lim, "Flexible wearable sensors for cardiovascular health monitoring," *Adv. Healthcare Mater.*, vol. 10, no. 17, Sep. 2021, Art. no. 2100116.

[22] C. Massaroni, M. Zaltieri, D. Lo Presti, A. Nicolò, D. Tosi, and E. Schena, "Fiber Bragg grating sensors for cardiorespiratory monitoring: A review," *IEEE Sensors J.*, vol. 21, no. 13, pp. 14069–14080, Jul. 2021.

[23] D. Lo Presti et al., "Fiber Bragg gratings for medical applications and future challenges: A review," *IEEE Access*, vol. 8, pp. 156863–156888, 2020.

[24] Y. Chee, J. Han, J. Youn, and K. Park, "Air mattress sensor system with balancing tube for unconstrained measurement of respiration and heart beat movements," *Physiol. Meas.*, vol. 26, no. 4, pp. 413–422, Aug. 2005.

[25] J. Di Tocco, L. Raiano, R. Sabbadini, C. Massaroni, D. Formica, and E. Schena, "A wearable system with embedded conductive textiles and an IMU for unobtrusive cardio-respiratory monitoring," *Sensors*, vol. 21, no. 9, p. 3018, Apr. 2021.

[26] D. Lo Presti, D. Bianchi, C. Massaroni, A. Gizzi, and E. Schena, "A soft and skin-interfaced smart patch based on fiber optics for cardiorespiratory monitoring," *Biosensors*, vol. 12, no. 6, p. 363, May 2022.

[27] L. Dziuda, F. W. Skibniewski, M. Krej, and J. Lewandowski, "Monitoring respiration and cardiac activity using fiber Bragg grating-based sensor," *IEEE Trans. Biomed. Eng.*, vol. 59, no. 7, pp. 1934–1942, Jul. 2012.

[28] K. Watanabe, T. Watanabe, H. Watanabe, H. Ando, T. Ishikawa, and K. Kobayashi, "Noninvasive measurement of heartbeat, respiration, snoring and body movements of a subject in bed via a pneumatic method," *IEEE Trans. Biomed. Eng.*, vol. 52, no. 12, pp. 2100–2107, Dec. 2005.

[29] E. Griffiths, T. S. Saponas, and A. J. B. Brush, "Health chair: Implicitly sensing heart and respiratory rate," in *Proc. ACM Int. Joint Conf. Pervasive Ubiquitous Comput.*, Sep. 2014, pp. 661–671.

[30] D. Lo Presti et al., "Cardio-respiratory monitoring in archery using a smart textile based on flexible fiber Bragg grating sensors," *Sensors*, vol. 19, no. 16, p. 3581, Aug. 2019.

[31] D. Lo Presti, F. Santucci, C. Massaroni, D. Formica, R. Setola, and E. Schena, "A multi-point heart rate monitoring using a soft wearable system based on fiber optic technology," *Sci. Rep.*, vol. 11, no. 1, p. 21162, Oct. 2021.

[32] Ł. Dziuda, F. W. Skibniewski, M. Krej, and P. M. Baran, "Fiber Bragg grating-based sensor for monitoring respiration and heart activity during magnetic resonance imaging examinations," *J. Biomed. Opt.*, vol. 18, no. 5, May 2013, Art. no. 057006.

[33] L. Dziuda, M. Krej, and F. W. Skibniewski, "Fiber Bragg grating strain sensor incorporated to monitor patient vital signs during MRI," *IEEE Sensors J.*, vol. 13, no. 12, pp. 4986–4991, Dec. 2013.

[34] F. de Tommasi, D. L. Presti, M. Carassiti, E. Schena, and C. Massaroni, "Smart mattress based on fiber Bragg grating sensors for respiratory monitoring: A feasibility test," in *Proc. IEEE Int. Workshop Metrolo. Ind. 4.0 IoT (MetroInd4.0 IoT)*, Jun. 2021, pp. 532–537.

[35] F. De Tommasi, D. L. Presti, M. A. Caponero, M. Carassiti, E. Schena, and C. Massaroni, "Smart mattress based on multipoint fiber Bragg gratings for respiratory rate monitoring," *IEEE Trans. Instrum. Meas.*, vol. 72, pp. 1–10, 2023.

[36] J. Hao, M. Jayachandran, P. L. Kng, S. F. Foo, P. W. A. Aung, and Z. Cai, "FBG-based smart bed system for healthcare applications," *Frontiers Optoelectron. China*, vol. 3, no. 1, pp. 78–83, Mar. 2010.

[37] P. Han et al., "Low-cost plastic optical fiber sensor embedded in mattress for sleep performance monitoring," *Opt. Fiber Technol.*, vol. 64, Jul. 2021, Art. no. 102541.

[38] J. Ben-Ari, E. Zimlichman, N. Adi, and P. Sorkine, "Contactless respiratory and heart rate monitoring: Validation of an innovative tool," *J. Med. Eng. Technol.*, vol. 34, nos. 7–8, pp. 393–398, Oct. 2010.

[39] R.-Y. Yang, A. Bendjoudi, N. Buard, and P. Boutouyrie, "Pneumatic sensor for cardiorespiratory monitoring during sleep," *Biomed. Phys. Eng. Exp.*, vol. 5, no. 5, Aug. 2019, Art. no. 055014.

[40] J. Ranta, T. Aittokoski, M. Tenhunen, and M. Alasaukko-Oja, "EMFIT QS heart rate and respiration rate validation," *Biomed. Phys. Eng. Exp.*, vol. 5, no. 2, Jan. 2019, Art. no. 025016.

[41] O. T. Inan et al., "Ballistocardiography and seismocardiography: A review of recent advances," *IEEE J. Biomed. Health Informat.*, vol. 19, no. 4, pp. 1414–1427, Jul. 2015.

[42] A. Othonos, "Fiber Bragg gratings," *Rev. Sci. Instrum.*, vol. 68, no. 12, pp. 4309–4341, Dec. 1997.

[43] W. Yan, S. Ma, H. Wang, and X. Zhang, "Fiber Bragg grating online packaging technology based on 3D printing," *Opt. Laser Technol.*, vol. 131, Nov. 2020, Art. no. 106443.

[44] D. L. Presti et al., "The effect of infill pattern and density on the response of 3-D-printed sensors based on FBG technology," *IEEE Sensors J.*, vol. 22, no. 20, pp. 19357–19365, Oct. 2022.

[45] F. De Tommasi, C. Romano, D. L. Presti, C. Massaroni, M. Carassiti, and E. Schena, "FBG-based soft system for assisted epidural anesthesia: Design optimization and clinical assessment," *Biosensors*, vol. 12, no. 8, p. 645, Aug. 2022.

[46] K. S. C. Kuang, R. Kenny, M. P. Whelan, W. J. Cantwell, and P. R. Chalker, "Embedded fibre Bragg grating sensors in advanced composite materials," *Compos. Sci. Technol.*, vol. 61, no. 10, pp. 1379–1387, Aug. 2001.

[47] C. Tavares et al., "Respiratory and heart rate monitoring using an FBG 3D-printed wearable system," *Biomed. Opt. Exp.*, vol. 13, no. 4, pp. 2299–2311, 2022.

[48] D. Lo Presti et al., "Wearable system based on flexible FBG for respiratory and cardiac monitoring," *IEEE Sensors J.*, vol. 19, no. 17, pp. 7391–7398, Sep. 2019.

[49] T. Erdogan, "Fiber grating spectra," *J. Lightw. Technol.*, vol. 15, no. 8, pp. 1277–1294, Aug. 1997.

[50] *Cardiac Monitors, Heart Rate Meters, and Alarms*, American National Standard ANSI/AAMI EC13:2002, Association for the Advancement of Medical Instrumentation, Arlington, VA, USA, 2002, pp. 1–87.

[51] C. A. R. Díaz et al., "A cost-effective edge-filter based FBG interrogator using catastrophic fuse effect micro-cavity interferometers," *Measurement*, vol. 124, pp. 486–493, Aug. 2018.

[52] C. A. R. Diaz et al., "Perrogator: A portable energy-efficient interrogator for dynamic monitoring of wavelength-based sensors in wearable applications," *Sensors*, vol. 19, no. 13, p. 2962, Jul. 2019.

Francesca De Tommasi (Student Member, IEEE) received the M.Sc. degree in biomedical engineering from the University Campus Bio-Medico di Roma (UCBM), Rome, Italy, in 2020, where she is currently the Ph.D. degree.

Her research interests focus on the development of fiber Bragg grating (FBG)-based measurement systems for biomedical applications.

Carlo Massaroni (Senior Member, IEEE) received the Ph.D. degree in biomedical engineering from the University Campus Bio-Medico di Roma (UCBM), Rome, Italy, in 2017.

He is currently an Assistant Professor with UCBM. His research interests include the design, development, and testing of wearable devices and contactless techniques, methods, and measuring systems for medical applications.

Michele Arturo Caponero received the bachelor's degree in physics from the University of Bari, Bari, Italy, in 1986.

He is a Researcher with the Photonics Micro and Nanostructures Laboratory, ENEA Research Center of Frascati, Frascati, Italy. His research interests include distributed fiber optic-based sensors for structural monitoring and interferometric technique's development.

Massimiliano Carassiti is an Associate Professore and an Anestesiologist with Fondazione Policlinico Universitario Campus Bio-Medico, Rome, Italy. His research interests include anesthesiology, intensive care medicine, and pain medicine and management.

Emiliano Schena (Senior Member, IEEE) received the Ph.D. degree in biomedical engineering from the University Campus Bio-Medico di Roma (UCBM), Rome, Italy, in 2009.

He is currently an Associate Professor with UCBM. His main research interests include systems for monitoring physiological parameters, application of fiber optic sensors in medicine, and laser ablation for cancer removal.

Daniela Lo Presti (Member, IEEE) received the Ph.D. degree from the Università Campus Bio-Medico di Roma, Rome, Italy, in 2021.

She is currently an Assistant Professor with the Unit of Measurements and Biomedical Instrumentation, University Campus Bio-Medico di Roma (UCBM), Rome, Italy. Her main research activities focus on the design, fabrication, and feasibility assessment of smart systems and wearables based on fiber optics technology for biomedical applications.

Open Access funding provided by 'Università "Campus Bio-Medico" di Roma' within the CRUI CARE Agreement